

# Robot-to-Robot Relative Pose Estimation using Humans as Markers

Md Jahidul Islam<sup>1</sup>, Jiawei Mo<sup>2</sup> and Junaed Sattar<sup>3</sup>

**Abstract**—In this paper, we propose a method to determine the 3D relative pose of pairs of communicating robots by using human pose-based key-points as correspondences. We adopt a ‘leader-follower’ framework where the leader robot detects and triangulates the key-points in its own frame of reference. Afterwards, the follower robots match the corresponding 2D projections on their respective calibrated cameras and find their relative poses by solving the perspective-n-point (PnP) problem. In the proposed method, we use the state-of-the-art pose detector named OpenPose for extracting the pose-based key-points pertaining to humans in the scene. Additionally, we design an efficient model for person re-identification and present an iterative optimization algorithm to refine the key-point correspondences based on their local structural similarities in the image space. We evaluate the performance of the proposed relative pose estimation method through a number of experiments conducted in terrestrial and underwater environments. Finally, we discuss the relevant operational challenges of this approach and analyze its feasibility for multi-robot cooperative systems in human-dominated social settings and in feature-deprived environments such as underwater.

## I. INTRODUCTION

Accurate computation of relative pose is essential in multi-robot estimation problems such as cooperative tracking, localization [1], planning, mapping [2], and more. Unless global positioning information (e.g., provided by GPS) is available, the robots need to estimate their positions and orientations relative to each other based on their *exteroceptive* sensory measurements and odometry [3] which is often noisy. This process is necessary for registering their measurements to a common frame of reference in order to maintain coordination. Therefore, robust estimation of robot-to-robot relative pose is crucial for deploying a team of robots in GPS-denied environments.

In a cooperative setting, robots with visual sensing capabilities solve the relative pose estimation problem by triangulating mutually visible local features and landmarks. A lack of salient features significantly affects the accuracy of this estimation [4], which eventually hampers the overall success of the operation. Such difficulties often arise in poor visibility conditions underwater due to a lower number of salient features and natural landmarks [5], [6]. Nevertheless, close proximity of human divers to robots is a fairly common occurrence in underwater applications [7]. In addition, humans are frequently present and clearly visible in many social scenarios [8], [9] where natural landmarks are not reliably identifiable (due to repeated textures, noisy

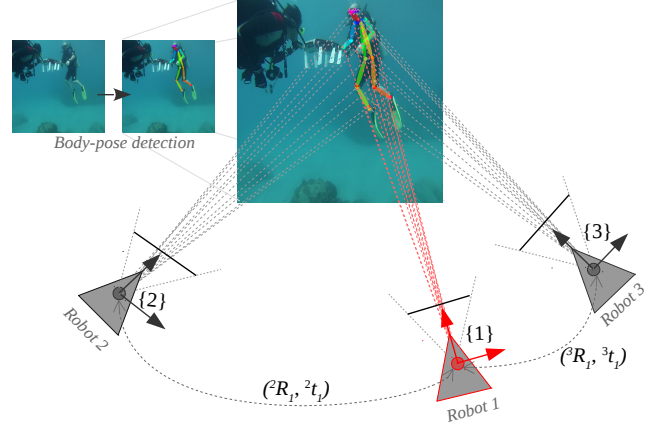


Fig. 1: A simplified illustration of 3D relative pose estimation between robot 1 and robot 2 (3). The robots know the transformations between their intrinsically calibrated cameras and respective global frames, i.e.,  $\{1\}$ ,  $\{2\}$ , and  $\{3\}$ . Robot 1 is considered as the leader (equipped with a stereo camera) and its pose in global coordinates ( ${}^1R_G, {}^1t_G$ ) is known. Robot 2 (3) finds its unknown global pose by cooperatively localizing itself relative to robot 1 using the human pose-based key-points as common landmarks.

visual conditions, etc.). Hence, the problem of having limited natural landmarks can be alleviated by using mutually visible humans as *markers* (i.e., features correspondences). Despite the potential, feasibility of using human presence or body-pose for robot-to-robot relative pose estimation has not been explored in the literature.

In this paper, we propose a method for computing six degree-of-freedom (6-DOF) robot-to-robot transformation between pairs of communicating robots by using mutually detected humans’ pose-based key-points as correspondences. As illustrated in Figure 1, we adopt a *leader-follower* framework where one of the robots (equipped with a stereo camera) is assigned as a leader. First, the leader robot detects and triangulates 3D positions of the key-points in its own frame of reference. Then the follower robot matches the corresponding 2D projections on its intrinsically calibrated camera and localizes itself by solving the perspective-n-point (PnP) problem [10]. It is to be noted that this entire process of *extrinsic calibration* is automatic and does not require prior knowledge about the robots’ initial positions. Additionally, it is straightforward to extend the leader-follower framework for multi-robot teams from the pairwise solutions. Furthermore, if the leader robot has global positioning information (i.e., has a GPS or an ultra-short baseline, or USBL, receiver), the follower robots can use that information to localize themselves in the global frame as well.

In addition to presenting the conceptual model and im-

\*This work is currently being reviewed at IROS 2019

The authors are with the Interactive Robotics and Vision Laboratory, Department of Computer Science and Engineering, University of Minnesota-Twin Cities, US.

E-mail: {<sup>1</sup>islam034, <sup>2</sup>moxxx066, <sup>3</sup>junaed}@umn.edu

plementation details, we provide efficient solutions to the practicalities involved in the proposed robot-to-robot pose estimation method. Specifically, we make the following contributions in this paper:

- 1) We use OpenPose [11] for detecting human body-poses in the image-space. Although it provides reliable detection performances, the extracted 2D key-points across different views do not necessarily associate as a correspondence. We solve this problem by designing an iterative optimization algorithm that refines the noisy key-points based on their local structural properties in respective images.
- 2) In addition, we exploit the structural similarities of each set of key-points and bundle their features in a hierarchical fashion for fast person re-identification (*i.e.*, association) across viewpoints.
- 3) Furthermore, we evaluate the proposed estimation method over a number of terrestrial and underwater experiments. We also analyze its feasibility in various multi-robot cooperative systems and discuss relevant operational considerations.

## II. RELATED WORK

The following sections present a brief discussion on the existing literature that are relevant to our problem of interest.

### A. Robot-to-robot Relative Pose Estimation

The problem of robot-to-robot relative pose estimation has been thoroughly studied for 2D planar robots, particularly using range and bearing sensors. Analytic solutions for determining 3-DOF robot-to-robot transformation using mutual distance and/or bearing measurements [3], [12] involve solving an over-determined system of nonlinear equations. Similar solutions for 3D case (*i.e.*, for determining 6-DOF transformation using inter-robot distance and/or bearing measurements) has been proposed as well [13], [14]. In practice, these analytic solutions are used as an initial estimate for the relative pose, and then iteratively refined using optimization techniques (*e.g.*, nonlinear weighted least-squares) in order to account for noisy observation and uncertainty in the robots' motion.

Robots that rely on visual perception (*i.e.*, use cameras as exteroceptive sensors) solve the relative pose estimation problem by triangulating mutually visible features and landmarks [15]. Therefore, it reduces to solving the PnP problem by using sets of 2D-3D correspondences between geometric features and their projections on respective image planes [10]. Although high-level geometric features (*e.g.*, lines, conics, etc.) have been proposed, point features are typically used in practice for relative pose estimation [16]. Moreover, PnP problem is solved either using iterative approaches by formulating the over-constrained system ( $n > 3$ ) as a nonlinear least-squares problem, or by using sets of three non-collinear points ( $n = 3$ ) in combination with Random Sample Consensus (RANSAC) [17] to remove outliers. In addition, vision-based approaches often use temporal-filtering methods, the extended Kalman-filter

(EKF) in particular, to reduce the effects of noisy measurements in order to provide near-optimal pose estimates [15], [16]. On the other hand, it is also common to simplify the relative pose estimation by attaching specially designed calibration-patterns on each robot [18]. However, it requires that the robots operate at a sufficiently close range, and remain mutually visible.

### B. Human Body-Pose Detection

The state-of-the-art methodologies can be categorized into the top-down and bottom-up approaches. The top-down approaches [19], [20] detect the humans in the image-space first and then perform localization and association of their body-parts. One major limitation of these approaches is that their running times are proportional to the number of persons in the image. In addition, robustness of the pose estimation largely depends on the accuracy of their person detectors. In contrast, the bottom-up approaches [11], [21] do not suffer from these two issues. However, they require solving a more computationally challenging inference problem of learning global contextual cues for simultaneous detection and association of the body parts.

The classical approaches [22], [23] use pictorial structures to model the appearance of human body-parts. A set of densely sampled shape descriptors are used for localizing the body-parts and then classifiers such as AdaBoost, SVMs, etc., are used for detection. Associating the detected body-parts are rather challenging, a mixture of tree-based models are typically used to learn separate pairwise relationships for different body-part configurations [24]. Graph-based connectivity models are then used to formulate the inference (association) as a graph-cut problem. Recently proposed approaches use Deep Neural Networks (DNNs) to learn the human pose detection from large training datasets in order to perform fast and accurate global inference. DeepPose [25], for instance, formulates the problem as a regression problem and uses a cascade of DNNs to learn the inference in a holistic fashion. On the other hand, OpenPose [11] jointly learns to detect and associate using pose machines [26]. In contrast to DNNs, each *module* of a pose machine is trained locally; the sequential predictions of these modules are then refined to perform a hierarchical joint inference. Such hierarchical structures facilitate fast inference for multi-person pose estimation in addition to achieving state-of-the-art detection performances. Due to these compelling reasons, we use OpenPose in this work.

### C. Human-aware Robot Control

Human-awareness is essential for autonomous mobile robots operating in social settings, and in human-robot collaborative applications. A large body of literature [7], [27], [8] and systems exist which focus on the areas of understanding human motion, instructions, behaviors, etc. Additionally, tracking human pose relative to the robot is particularly common in applications such as person tracking [28], following [8], collaborative manipulation [29], behavior imitation [30], etc. However, the feasibility of using

humans' presence or their body-poses as markers for robot-to-robot relative pose estimation has not been explored in the literature, which we attempt to address in this work.

### III. METHODOLOGY

The proposed robot-to-robot relative pose estimation method incorporates a number of computational components: detection of human body-poses in images captured from different views (by leader and follower robots), pair-wise association of the detected humans across multiple images, geometric refinement of the key-point correspondences, and 3D pose estimation of the follower robot (relative to the leader) using 2D-3D correspondences. We now elaborate their methodologies in the following sections.

#### A. Human Body-Pose Detection

We use OpenPose [11] for real-time multi-human 2D keypoint detection in images. It is an open-source library<sup>1</sup> originally written in C++ using Caffe and OpenCV libraries. We use a Tensorflow implementation<sup>2</sup> based on the 'MobileNet model' that provides faster inference compared to the original model. Specifically, it processes a  $368 \times 368$  image in  $180ms$  on a Jetson TX2 device<sup>3</sup>, whereas the original model (also known as the 'CMU model') takes multiple seconds.

OpenPose generates 18 annotated 2D key-points pertaining to the nose, neck, shoulders, elbows, wrists, hips, knees, ankles, eyes, and ears of a human body. As shown in Figure 2, a subset of these key-points and their pair-wise anatomical relationships are generated for each human. We represent the key-points generated by OpenPose in an image  $I$  by an  $N_I \times 18$  array where  $N_I$  is the number of humans (detected in the image); that is, each row contains 18 ordered key-points for a particular person. Specifically,

$$\mathbf{KP}(I) = \{h_{ij}\}, \quad i \in 1 : N_I, \quad j \in 1 : 18$$

If a particular key-point is not detected, then the values are left as  $(-1, -1)$ . Additionally, we configure  $\mathbf{KP}(I)$  in a way that the first row belongs to the left-most person, and gradually the last row belongs to the right-most person in the image; it is achieved by sorting the rows based on the average of its non-negative  $x$ -coordinates. This way of formatting the key-points helps to speed-up the process of associating correspondences between  $\mathbf{KP}(I_{leader})$  and  $\mathbf{KP}(I_{follower})$ .

In order to establish key-point correspondences between mutually visible humans in the scene, the rows of  $\mathbf{KP}(I_{leader})$  and  $\mathbf{KP}(I_{follower})$  need to be associated. That is, the follower robot needs to make sure that it is pairing the key-points of the *same* individuals. This is important because in practice they might be looking at different individuals, or same individuals in a different spatial order. Associating multiple persons across different images is a well-studied problem known as *person re-identification*.

<sup>1</sup>[github.com/CMU-Perceptual-Computing-Lab/openpose](https://github.com/CMU-Perceptual-Computing-Lab/openpose)

<sup>2</sup>[github.com/ildoonet/tf-pose-estimation](https://github.com/ildoonet/tf-pose-estimation)

<sup>3</sup>Jetson TX2 is a single-board super-computer by NVIDIA, widely used in mobile robots for deep visual computing.

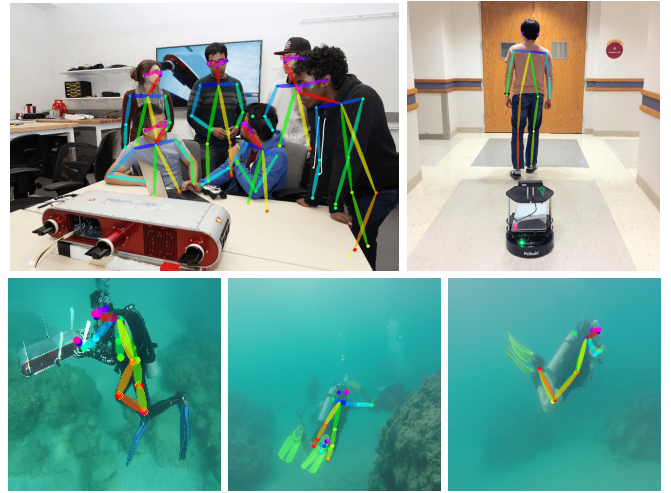


Fig. 2: Multi-human 2D body-pose detection using OpenPose in various human-robot collaborative settings.

#### B. Person Re-identification using Hierarchical Similarities

Although a number of existing deep visual models provide good solutions for person re-identification [31], [32], we design a simple and efficient model in order to meet the real-time on-board computational constraints. The intuition is to avoid using a computationally demanding feature extractor by making use of the hierarchical anatomical structures that are already embedded in the key-points. First, we bundle the subsets of key-points in several spatial bounding-boxes (Bbox) as follows:

- Face Bbox: nose, eyes, and ears
- Upper-body Bbox: neck, shoulders, and hips
- Lower-body Bbox: hips, knees, and ankles
- Left-arm Bbox: left shoulder, elbow, and wrist
- Right-arm Bbox: right shoulder, elbow, and wrist
- Full-body Bbox: encloses all the key-points

Figure 3 illustrates the spatial hierarchy of these bounding boxes and their corresponding key-points. They are extracted by spanning the corresponding key-points' coordinate values in both  $x$  and  $y$  dimensions. We use an offset (of additional 10% length) in each dimension in order to capture more spatial information around the key-points. A bounding box is discarded if its area is below an empirically chosen threshold; this happens when the corresponding body-part is not detected or its resolution is too small to be informative.

Once these bounding boxes are extracted, we use the structural properties of their respective image-patches as features for person re-identification; specifically, we compare the structural similarities [33] between image patches pertaining to face, upper-body, lower-body, left-arm and right-arm, and the full body of a person. Based on their aggregated similarities, we evaluate the pair-wise association between each person seen by the leader (in  $I_{leader}$ ) and by the follower (in  $I_{follower}$ ).

The structural similarity [33] for a particular pair of single-channel rectangular image-patches ( $\mathbf{x}, \mathbf{y}$ ) is evaluated based on three properties: luminance ( $l$ ), contrast ( $c$ ), and structure

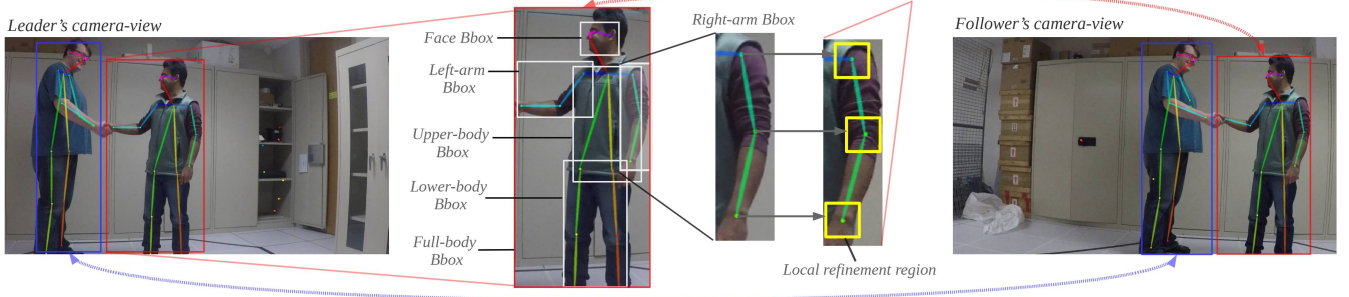


Fig. 3: An illustration of how the hierarchical body-parts are extracted for person re-identification based on their structural similarities; once the persons are associated, the pair-wise key-points are refined and used as correspondences.

(s). The standard way of computing these are:

$$l(\mathbf{x}, \mathbf{y}) = \frac{2\mu_{\mathbf{x}}\mu_{\mathbf{y}}}{\mu_{\mathbf{x}}^2 + \mu_{\mathbf{y}}^2}; c(\mathbf{x}, \mathbf{y}) = \frac{2\sigma_{\mathbf{x}}\sigma_{\mathbf{y}}}{\sigma_{\mathbf{x}}^2 + \sigma_{\mathbf{y}}^2}; s(\mathbf{x}, \mathbf{y}) = \frac{\sigma_{\mathbf{xy}}}{\sigma_{\mathbf{x}}\sigma_{\mathbf{y}}}$$

Here,  $\mu_{\mathbf{x}}$  ( $\mu_{\mathbf{y}}$ ) denotes the mean of image patch  $\mathbf{x}$  ( $\mathbf{y}$ ),  $\sigma_{\mathbf{x}}^2$  ( $\sigma_{\mathbf{y}}^2$ ) denotes the variance of  $\mathbf{x}$  ( $\mathbf{y}$ ), and  $\sigma_{\mathbf{xy}}$  denotes the cross-correlation between  $\mathbf{x}$  and  $\mathbf{y}$ . The structural similarity metric (SSIM) is then defined as:

$$SSIM(\mathbf{x}, \mathbf{y}) = l(\mathbf{x}, \mathbf{y})c(\mathbf{x}, \mathbf{y})s(\mathbf{x}, \mathbf{y}) = \frac{2\mu_{\mathbf{x}}\mu_{\mathbf{y}}}{\mu_{\mathbf{x}}^2 + \mu_{\mathbf{y}}^2} \cdot \frac{2\sigma_{\mathbf{xy}}}{\sigma_{\mathbf{x}}^2 + \sigma_{\mathbf{y}}^2}$$

In order to ensure numeric stability, two constants  $c_1 = (255k_1)^2$  and  $c_2 = (255k_2)^2$  are added as follows:

$$SSIM(\mathbf{x}, \mathbf{y}) = \left( \frac{2\mu_{\mathbf{x}}\mu_{\mathbf{y}} + c_1}{\mu_{\mathbf{x}}^2 + \mu_{\mathbf{y}}^2 + c_1} \right) \left( \frac{2\sigma_{\mathbf{xy}} + c_2}{\sigma_{\mathbf{x}}^2 + \sigma_{\mathbf{y}}^2 + c_2} \right) \quad (1)$$

We use  $k_1 = 0.01$ ,  $k_2 = 0.03$ , and an  $8 \times 8$  sliding window in our implementation. Additionally, we resize the patches extracted from  $I_{leader}$  so that their corresponding pairs in  $I_{follower}$  have the same dimensions. Then, we apply Equation 1 on every channel ( $R, G, B$ ) and use their average value as the similarity metric (on a scale of  $[0, 1]$ ). Specifically, we use this metric for person re-identification as follows:

- We only consider the mutually visible body-parts for evaluating pair-wise SSIM values (and take their average). This choice is important to enforce meaningful comparisons; otherwise, it is equivalent to using only the full-body Bbox, which we found to be highly inaccurate.
- Each person in  $I_{follower}$  is associated with the most similar person (*i.e.*, corresponds to the maximum SSIM value) in  $I_{leader}$ . However, the association is discarded if the maximum SSIM value is less than a predefined threshold ( $\delta_{min}$ ); we use  $\delta_{min} = 0.4$  in our implementation. This reduces the risk of inaccurate associations, particularly when there are mutually exclusive people in the scene.

### C. Key-point Refinement

Once the specific persons are identified, *i.e.*, the rows of  $KP(I_{leader})$  and  $KP(I_{follower})$  are associated, the mutually visible key-points are paired together to form correspondences. Although the key-points are ordered and OpenPose

localizes them reasonably well, they cannot be readily used as geometric correspondences due to perspective distortions and noise. We attempt to solve this problem by designing an iterative optimization algorithm that refines the noisy correspondences based on their structural properties in a  $32 \times 32$  neighborhood. By denoting  $\phi_I(\mathbf{p})$  as the  $32 \times 32$  image-patch centered at  $\mathbf{p} = [p_x, p_y]^T$  in image  $I$ , we define a loss function for each correspondence ( $\mathbf{p}_l \in I_{leader}, \mathbf{p}_f \in I_{follower}$ ) as follows:

$$L(\mathbf{p}_l, \mathbf{p}_f) = 1 - SSIM(\phi_{I_{leader}}(\mathbf{p}_l), \phi_{I_{follower}}(\mathbf{p}_f)) \quad (2)$$

Then, we refine each initial key-point correspondence ( $\mathbf{p}_l^0, \mathbf{p}_f^0$ ) by minimizing the following function:

$$\mathbf{p}_f^* = \underset{\mathbf{p}}{\operatorname{argmin}} L(\mathbf{p}_l^0, \mathbf{p}) \quad \text{s. t.} \quad \|\mathbf{p} - \mathbf{p}_f^0\|_{\infty} < 32 \quad (3)$$

As Equation 3 suggests, we fix  $\mathbf{p}_l = \mathbf{p}_l^0$  and refine  $\mathbf{p}_f = \mathbf{p}_f^0$  to maximize  $SSIM(\phi_{I_{leader}}(\mathbf{p}_l), \phi_{I_{follower}}(\mathbf{p}_f))$ . We use a refinement region of  $32 \times 32$  in our implementation, whereas the resolution of  $I_{follower}$  is  $640 \times 480$ . In addition, we use a gradient-based refinement; specifically, we perform the following iterative update:

$$\mathbf{p}_f^{t+1} = \mathbf{p}_f^t - \eta \cdot \nabla L(\mathbf{p}_l^0, \mathbf{p}_f^t) \quad (4)$$

Similar formulation using SSIM-based loss function for optimization is fairly standard in literature [34], [35]. We follow the procedures suggested in [35] for computing the gradient of SSIM. In practice, we stack all the key-points and their gradients (separately) in order to perform the optimization at once. In addition, a fixed learning rate of  $\eta = 0.003$  and a maximum iteration of 100 is used in our implementation.

### D. Robot-to-robot Pose Estimation

Once the mutually visible key-points are associated and refined, the follower robot uses the corresponding 3D positions (provided by the leader) to estimate its relative pose by solving a PnP problem. Thus, we require that the leader robot is equipped with a stereo camera (or a RGBD camera) so that it can triangulate using epipolar constraints (or use the depth sensor) in order to represent the key-points in 3D.

Let  $\mathbf{x}_l$  denote the 3D locations of the key-points in leader's coordinate frame, and  $\mathbf{p}_f$  denote their corresponding 2D



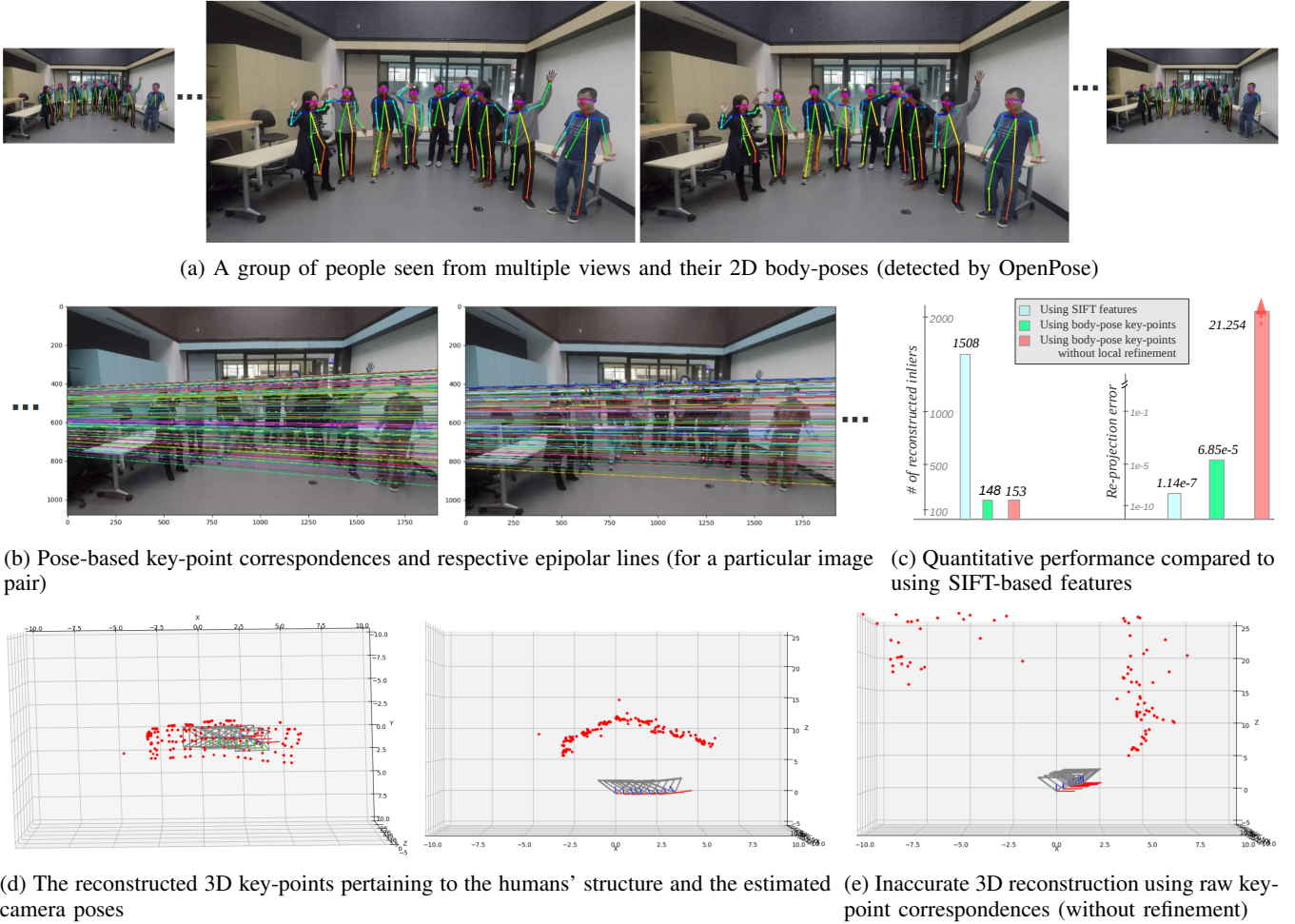


Fig. 4: Results of estimating *structure-from-motion* using only human pose-based key-points as features.

projections on the follower's camera. Then, assuming the cameras are synchronized, the PnP problem is formulated as follows:

$$\mathbf{T}_f^l = \underset{\mathbf{T}_f^l}{\operatorname{argmin}} \|\mathbf{p}_f - \mathbf{K}_f \mathbf{T}_f^l \mathbf{x}_l\|^2 \quad (5)$$

Here,  $\mathbf{K}_f$  is the intrinsic matrix of the follower's camera and  $\mathbf{T}_f^l$  is its 6-DOF transformation relative to the leader. In our implementation, we follow the standard iterative solution for PnP using RANSAC [10].

#### IV. EXPERIMENTAL ANALYSIS

We conduct a number of experiments with 2D and 3D robots to evaluate the applicability and performance of the relative pose estimation method. We present the experiments, analyze the results, and discuss various operational considerations in the following sections.

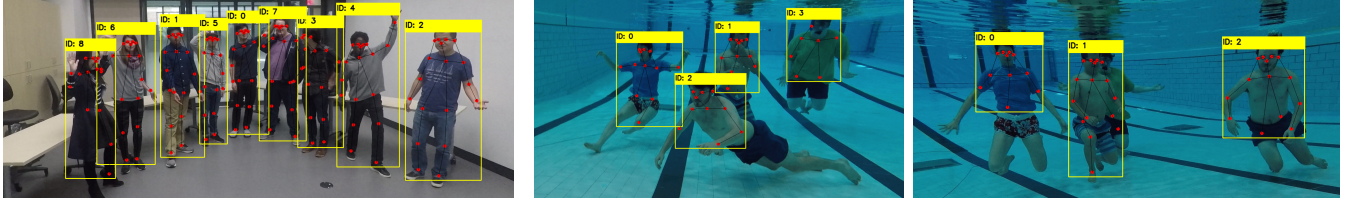
##### A. Proof of Concept: Structure from Motion

We perform experiments to validate that the human pose-based key-points can be used as reliable correspondences for relative pose estimation. As illustrated in Figure 4(a), we emulate an experimental set-up for *structure from motion* with humans; we use an intrinsically calibrated monocular

camera to capture a group of nine (static) people from multiple views. Here, the goal is to estimate the camera poses and reconstruct the 3D structures of the humans using only their body-poses as features.

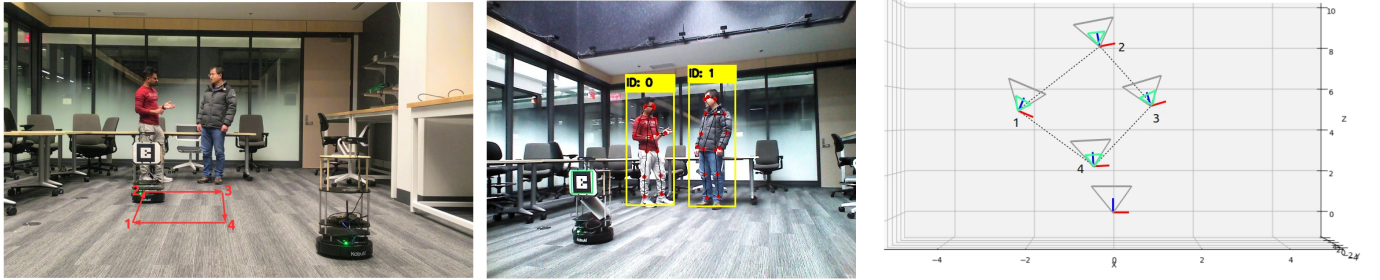
First, we use the proposed person re-identification and key-point refinement processes in order to obtain the feature correspondences. Then, we follow the standard procedures for structure from motion [36]: fundamental matrix computation (8-point algorithm with RANSAC), camera pose estimation (Cheirality constraint), and linear triangulation. Finally, the triangulated 3D points and camera poses are refined using bundle adjustment. We follow the same procedure using SIFT-features for comparison.

As demonstrated in Figure 4(d), the structure of the humans are reconstructed and camera poses are estimated with reasonable accuracy (*e.g.*, with an average re-projection error of  $6.85e^{-5}$  pixels). In addition, Figure 4(c)-(e) demonstrate the necessity and effectiveness of the proposed key-point refinement method. Furthermore, as shown in Figure 5, the proposed person re-identification method can accurately associate specific persons across multiple images, even when the humans are partially occluded, or their pose changes significantly.



(a) The uniquely identified persons for a particular image (from the experiment shown in Figure 4) (b) The persons are accurately associated even though there are significant changes in their poses

Fig. 5: Results for the proposed person re-identification method (an unique identifier is assigned to each association).



(a) The follower robot takes four measurements on a rectangular pattern (b) The leader robot detects the pose-based key-points and shares the 3D leader locations (c) Estimated poses of the follower relative to the leader (the green cones represent the respective ground-truths)

Fig. 6: An experiment to evaluate the accuracy of 2D relative pose estimation with two planar robots and two mutually visible humans.

### B. Ground Experiments: 3-DOF Pose Estimation

We perform an experiment with two planar robots as demonstrated in Figure 6. The robot with an Alvar AR-tag<sup>4</sup> on its back is used as the follower robot while the other robot is used as the leader. The static leader uses its RGBD camera to detect the human pose-based 2D key-points and associates the corresponding depth information in order to represent them in 3D. On the other hand, the follower robot uses this information to localize itself relative to the robot by following the proposed method. We take four such measurements on a rectangular pattern (Figure 6(a)) and evaluate the relative pose estimates with respect to the ground-truths (Figure 6(c)). We have observed 0.0475% average error in translation and a 0.8625° average error in rotation, which are reasonably accurate.

### C. Underwater Experiments: 6-DOF Pose Estimation

We also perform field experiments for 3D relative pose estimation with underwater robots. Figure 7 shows the setup of a particular experiment; here, we capture body-poses of multiple humans in the scene from different perspectives using multiple underwater robots (and cameras). Then, we follow the proposed method to estimate their 6-DOF transformations relative to a leader.

At first, the pose-based key-points are detected and triangulated by the leader's stereo cameras. The stereo correspondences are obtained by using the proposed person re-identification and key-point refinement processes; then

the epipolar constraints are used to remove outliers. Subsequently, the 3D key-point locations and their 2D projections in respective follower robots' cameras are used to find their relative poses. Figure 8 illustrates the robots' perspectives, annotated key-points, and their (estimated) 3D poses.



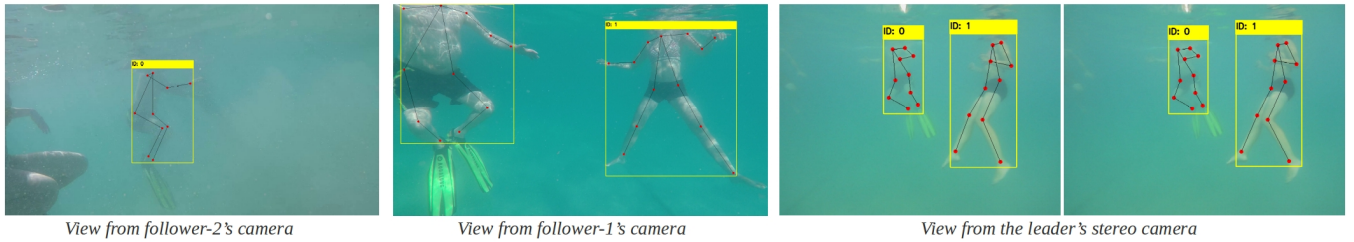
Fig. 7: An aerial view of the underwater experiment; multiple robots and cameras are used to capture the humans' from different perspectives.

### D. Discussion: Operational Challenges and Practicalities

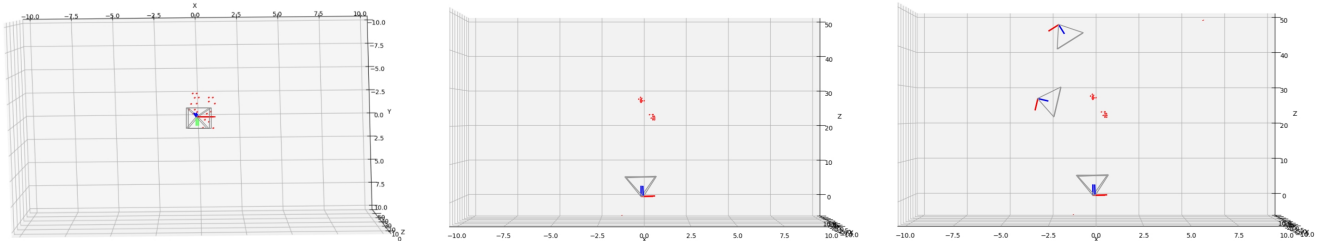
There are a few operational considerations and challenges involved for practical implementations of the proposed pose estimation method. We now discuss these aspects and their possible solutions based on our experimental findings.

1) *Synchronized Cooperation*: A major operational requirement of multi-robot cooperative systems is the ability to register synchronized measurements in a common frame of reference. However, it is quite challenging in practice. For

<sup>4</sup>The AR-tag is used to obtain the follower robot's ground-truth relative pose for comparison.



(a) A group of people seen from multiple perspectives; the detected key-points and their associations are annotated in respective images



(b) Stereo triangulation of the key-points (by the leader)

(c) Estimated relative poses of the followers

Fig. 8: An underwater experiment for 3D relative pose estimation using one leader and two follower robots.

problems such as ours, an effective solution is to maintain a buffer of time-stamped measurements and register them as a batch using a temporal *sliding-window*. The follower robots in particular can use such techniques to find their relative poses at regular time intervals. However, the challenge still remains in finding the instantaneous relative poses, especially when both robots are in motion.

2) *Person Association and Key-point Refinement*: As mentioned, correct person association and key-point refinement are vital for accurate pose estimation. Although there are good solutions for these problems in the literature, those are often computationally too demanding for real-time applications. For example, the state-of-the-art appearance-based person re-identification models [31], [32] perform reasonably well in practice. However, we have found that they require multiple seconds to associate more than two persons in a single frame. Hence, there is a trade-off between accuracy and running-time, which led us to design the methodologies proposed in Section III-B and III-C.

3) *Other Issues and Limitations*: We have observed a couple of practical issues during the experiments. First, the presence of multiple humans in the scene is needed to ensure reliable pose estimation performances. We have found that two or more mutually visible humans are ideal for establishing a large set of reliable correspondences. In addition, we have found that the pose estimation performance is affected by the relative viewing angle; specifically, it often fails to find correct associations when the  $\angle_{\text{leader-human-follower}}$  is larger than (approximately)  $135^\circ$ . This results in a situation where the robots are exclusively looking at the opposite sides of the person without enough common key-points.

## V. CONCLUSIONS AND FUTURE WORK

In this paper, we explore the feasibility of using human body-poses as markers to establish reliable multi-view geometric correspondences and eventually solve the robot-to-robot relative pose estimation problem. First, we use OpenPose for extracting the pose-based 2D key-points pertaining to the humans in the scene. Then, we associate the humans seen from multiple views using an efficient person re-identification model. Subsequently, we refine the key-point correspondences using an iterative optimization algorithm based on their local structural similarities in the image-space. Finally, we use the 3D locations of the key-points (triangulated by the leader robot) and their corresponding 2D projections (seen by the follower robot) to formulate a PnP problem and solve for the unknown pose of the follower robot relative to the leader. We perform extensive experiments in terrestrial and underwater environments in order to investigate the applicability of the proposed relative pose estimation method; the experimental results validate its effectiveness both for 2D and 3D robots. We also discuss the relevant operational challenges and propose efficient solutions to deal with them.

In the future, we seek to improve the end-to-end running time of the proposed system and plan to use it in practical applications such as multi-robot convoying, cooperative source-to-destination planning, etc. Additionally, we aim to investigate the applicability of DensePose [37] in our work which can potentially provide significantly more key-point correspondences per-person compared to OpenPose.

## ACKNOWLEDGEMENTS

We would like to thank Hyun Soo Park (Assistant Professor, University of Minnesota) for his valuable insights which immensely enriched this paper. We gratefully acknowledge the support of the MnDrive initiative and thank NVIDIA



Corporation for donating two Titan-class GPUs for this research. In addition, we are grateful to the Bellairs Research Institute of Barbados for providing us with the facilities for field experiments; we also acknowledge our colleagues at the IRVLAB and the participants of the 2019 Marine Robotics Sea Trials for their assistance in collecting data and conducting the experiments.

## REFERENCES

- [1] I. M. Rekleitis, G. Dudek, and E. E. Milios, “Multi-robot Cooperative Localization: A Study of Trade-offs Between Efficiency and Accuracy,” in *Proc. of the IEEE/RSJ International Conference on Intelligent Robots and Systems (IROS)*, vol. 3. IEEE, 2002, pp. 2690–2695.
- [2] S. Se, D. G. Lowe, and J. J. Little, “Vision-based Global Localization and Mapping for Mobile Robots,” *IEEE Transactions on Robotics (TRO)*, vol. 21, no. 3, pp. 364–375, 2005.
- [3] X. S. Zhou and S. I. Roumeliotis, “Robot-to-robot Relative Pose Estimation from Range Measurements,” *IEEE Transactions on Robotics (TRO)*, vol. 24, no. 6, pp. 1379–1393, 2008.
- [4] C. Valgren and A. J. Lilienthal, “SIFT, SURF & Seasons: Appearance-based Long-term Localization in Outdoor Environments,” *Robotics and Autonomous Systems*, vol. 58, no. 2, pp. 149–156, 2010.
- [5] H. Damron, A. Q. Li, and I. Rekleitis, “Underwater Surveying via Bearing only Cooperative Localization,” in *Proc. of the IEEE/RSJ International Conference on Intelligent Robots and Systems (IROS)*. IEEE, 2018, pp. 3957–3963.
- [6] J. Sattar, G. Dudek, O. Chiu, I. Rekleitis, P. Giguere, A. Mills, N. Plamondon, C. Prahacs, Y. Girdhar, M. Nahon *et al.*, “Enabling Autonomous Capabilities in Underwater Robotics,” in *Proc. of the IEEE/RSJ International Conference on Intelligent Robots and Systems (IROS)*. IEEE, 2008, pp. 3628–3634.
- [7] M. J. Islam, M. Ho, and J. Sattar, “Understanding Human Motion and Gestures for Underwater Human-Robot Collaboration,” *Journal of Field Robotics (JFR)*, pp. 1–23, 2018.
- [8] M. J. Islam, J. Hong, and J. Sattar, “Person Following by Autonomous Robots: A Categorical Overview,” *arXiv preprint arXiv:1803.08202*, 2018.
- [9] R. Kümmerle, M. Ruhnke, B. Steder, C. Stachniss, and W. Burgard, “A Navigation System for Robots Operating in Crowded Urban Environments,” in *Proc. of the IEEE International Conference on Robotics and Automation (ICRA)*. IEEE, 2013, pp. 3225–3232.
- [10] Y. Zheng, Y. Kuang, S. Sugimoto, K. Astrom, and M. Okutomi, “Revisiting the PnP Problem: A Fast, General and Optimal Solution,” in *Proc. of the IEEE International Conference on Computer Vision (ICCV)*, 2013, pp. 2344–2351.
- [11] Z. Cao, T. Simon, S.-E. Wei, and Y. Sheikh, “Realtime Multi-person 2d Pose Estimation using Part Affinity Fields,” in *IEEE Conference on Computer Vision and Pattern Recognition (CVPR)*, 2017, pp. 7291–7299.
- [12] N. Trawny and S. I. Roumeliotis, “On the Global Optimum of Planar, Range-based Robot-to-robot Relative Pose Estimation,” in *Proc. of the IEEE International Conference on Robotics and Automation (ICRA)*. IEEE, 2010, pp. 3200–3206.
- [13] X. S. Zhou and S. I. Roumeliotis, “Determining the Robot-to-robot 3D Relative Pose using Combinations of Range and Bearing Measurements (Part II),” in *IEEE International Conference on Robotics and Automation (ICRA)*. IEEE, 2011, pp. 4736–4743.
- [14] N. Trawny, X. S. Zhou, K. Zhou, and S. I. Roumeliotis, “Inter-robot transformations in 3D,” *IEEE Transactions on Robotics (TRO)*, vol. 26, no. 2, pp. 226–243, 2010.
- [15] J. Wang and W. J. Wilson, “3D Relative Position and Orientation Estimation using Kalman Filter for Robot Control,” in *Proc. of the IEEE International Conference on Robotics and Automation (ICRA)*. IEEE, 1992, pp. 2638–2645.
- [16] F. Janabi-Sharifi and M. Marey, “A Kalman-filter-based Method for Pose estimation in Visual Servoing,” *IEEE transactions on Robotics (TRO)*, vol. 26, no. 5, pp. 939–947, 2010.
- [17] M. A. Fischler and R. C. Bolles, “Random Sample Consensus: A Paradigm for Model Fitting with Applications to Image Analysis and Automated Cartography,” *Communications of the ACM*, vol. 24, no. 6, pp. 381–395, 1981.
- [18] I. Rekleitis, D. Meger, and G. Dudek, “Simultaneous Planning, Localization, and Mapping in a Camera Sensor Network,” *Robotics and Autonomous Systems*, vol. 54, no. 11, pp. 921–932, 2006.
- [19] G. Gkioxari, B. Hariharan, R. Girshick, and J. Malik, “Using K-poselets for Detecting People and Localizing their Keypoints,” in *Proc. of the IEEE Conference on Computer Vision and Pattern Recognition (CVPR)*, 2014, pp. 3582–3589.
- [20] L. Pishchulin, A. Jain, M. Andriluka, T. Thormählen, and B. Schiele, “Articulated People Detection and Pose Estimation: Reshaping the Future,” in *Proc. of the IEEE Conference on Computer Vision and Pattern Recognition (CVPR)*. IEEE, 2012, pp. 3178–3185.
- [21] L. Pishchulin, E. Insafutdinov, S. Tang, B. Andres, M. Andriluka, P. V. Gehler, and B. Schiele, “DeepCut: Joint Subset Partition and Labeling for Multi Person Pose Estimation,” in *Proc. of the IEEE Conference on Computer Vision and Pattern Recognition (CVPR)*, 2016, pp. 4929–4937.
- [22] M. Andriluka, S. Roth, and B. Schiele, “Pictorial Structures Revisited: People Detection and Articulated Pose Estimation,” in *Proc. of the IEEE Conference on Computer Vision and Pattern Recognition (CVPR)*. IEEE, 2009, pp. 1014–1021.
- [23] V. Ferrari, M. Marin-Jimenez, and A. Zisserman, “Progressive Search Space Reduction for Human Pose Estimation,” in *Proc. of the IEEE Conference on Computer Vision and Pattern Recognition (CVPR)*. IEEE, 2008, pp. 1–8.
- [24] S. Johnson and M. Everingham, “Learning Effective Human Pose Estimation from Inaccurate Annotation,” in *Proc. of the IEEE Conference on Computer Vision and Pattern Recognition (CVPR)*. IEEE, 2011, pp. 1465–1472.
- [25] A. Toshev and C. Szegedy, “DeepPose: Human Pose Estimation via Deep Neural Networks,” in *Proc. of the IEEE Conference on Computer Vision and Pattern Recognition (CVPR)*, 2014, pp. 1653–1660.
- [26] V. Ramakrishna, D. Munoz, M. Hebert, J. A. Bagnell, and Y. Sheikh, “Pose Machines: Articulated Pose Estimation via Inference Machines,” in *Proc. of the European Conference on Computer Vision (ECCV)*. Springer, 2014, pp. 33–47.
- [27] R. Mead and M. J. Matarić, “Autonomous Human-robot Proxemics: Socially aware Navigation based on Interaction Potential,” *Autonomous Robots*, vol. 41, no. 5, pp. 1189–1201, 2017.
- [28] M. Montemerlo, S. Thrun, and W. Whittaker, “Conditional Particle Filters for Simultaneous Mobile Robot Localization and People-tracking,” in *Proc. of the IEEE International Conference on Robotics and Automation (ICRA)*, vol. 1. IEEE, 2002, pp. 695–701.
- [29] J. Mainprice and D. Berenson, “Human-robot Collaborative Manipulation Planning using Early Prediction of Human Motion,” in *Proc. of the IEEE/RSJ International Conference on Intelligent Robots and Systems (IROS)*. IEEE, 2013, pp. 299–306.
- [30] J. Lei, M. Song, Z.-N. Li, and C. Chen, “Whole-body Humanoid Robot Imitation with Pose Similarity Evaluation,” *Signal Processing*, vol. 108, pp. 136–146, 2015.
- [31] E. Ahmed, M. Jones, and T. K. Marks, “An Improved Deep Learning Architecture for Person Re-identification,” in *Proc. of the IEEE Conference on Computer Vision and Pattern Recognition (CVPR)*, 2015, pp. 3908–3916.
- [32] W. Li, R. Zhao, T. Xiao, and X. Wang, “Deepreid: Deep Filter Pairing Neural Network for Person Re-identification,” in *Proc. of the IEEE Conference on Computer Vision and Pattern Recognition (CVPR)*, 2014, pp. 152–159.
- [33] Z. Wang, A. C. Bovik, H. R. Sheikh, E. P. Simoncelli *et al.*, “Image Quality Assessment: from Error Visibility to Structural Similarity,” *IEEE Transactions on Image Processing*, vol. 13, no. 4, pp. 600–612, 2004.
- [34] D. Otero and E. R. Vrscay, “Solving Optimization Problems that Employ Structural Similarity as the Fidelity Measure,” in *Proc. of the International Conference on Image Processing, Computer Vision, and Pattern Recognition (IPCV)*, 2014, p. 1.
- [35] A. N. Avanaki, “Exact Global Histogram Specification Optimized for Structural Similarity,” *Optical Review*, vol. 16, no. 6, pp. 613–621, 2009.
- [36] R. Hartley and A. Zisserman, *Multiple View Geometry in Computer Vision*. Cambridge University Press, 2003.
- [37] R. Alp Güler, N. Neverova, and I. Kokkinos, “DensePose: Dense Human Pose Estimation in the Wild,” in *Proc. of the IEEE Conference on Computer Vision and Pattern Recognition (CVPR)*, 2018, pp. 7297–7306.